INDERSCIENCE PUBLISHERS
Linking academia, business and industry through research

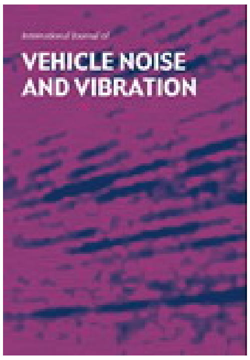

International Journal of Vehicle Noise and Vibration

ISSN online: 1479-148X - ISSN print: 1479-1471
https://www.inderscience.com/ijvnv

A comparative study of properties of natural rubber and polyurethane-based powertrain mount on electric vehicle NVH performance

Sandip Hazra, K. Janardhan Reddy

DOI: 10.1504/IJVNV.2022.10050577

Article History:

Received:	01 June 2021
Accepted:	16 December 2021
Published online:	16 September 2022

Copyright © Inderscience Enterprises Ltd.

A comparative study of properties of natural rubber and polyurethane-based powertrain mount on electric vehicle NVH performance

Sandip Hazra

Engineering Research Center (ERC),
Tata Motors Ltd.,
Pimpri, Pune – 411018, India
Email: shazra11@yahoo.com

K. Janardhan Reddy*

School of Mechanical Engineering (SMEC),
Vellore Institute of Technology – Chennai,
Kelambakkam – Vandalur Rd., Chennai,
Tamil Nadu – 600127, India
Email: kjanardhanreddy@vit.ac.in
*Corresponding author

Abstract: Natural rubber (NR) is widely used in powertrain mount applications in an internal combustion engine (ICE) and electric vehicle (EV) for its superior mechanical properties. Polyurethane (PU) is generally used as a bump stopper application under suspension in passenger cars for better ride and handling management due to its soft entry and better durability for its compressible behaviour. However, polyurethane application is gradually adopted in electric vehicle powertrain mounting systems where the specific dynamic properties are used to control the transfer of high motor torque reaction force during sudden acceleration. In this paper, properties like dynamic stiffness, creep, the durability of NR and PU are compared for application in powertrain mounting in the electric vehicle. The dynamic stiffness at low and high amplitude is discussed for both materials. The overall noise, vibration and harshness (NVH) and durability benefit of PU material in electric vehicle application are discussed in this paper.

Keywords: electric vehicle; EV; engine mount; dynamic stiffness; natural rubber; polyurethane.

Reference to this paper should be made as follows: Hazra, S. and Reddy, K.J. (2022) 'A comparative study of properties of natural rubber and polyurethane-based powertrain mount on electric vehicle NVH performance', *Int. J. Vehicle Noise and Vibration*, Vol. 18, Nos. 1/2, pp.22–40.

Biographical notes: Sandip Hazra currently working as the Deputy General Manager in Engineering Research Center, Tata Motors. He received his Master's degree from the IIT, Varanasi, India, in 2002. He has 20 years of professionalism in automotive design. His industrial experience includes working for Maruti Suzuki India Ltd., Renault Nissan Technical Center, and Tata Motors Ltd. His research interests are in product design, electric and hybrid driving technology, NVH technology for powertrain mount systems and vehicle driving dynamics.

Copyright © 2022 Inderscience Enterprises Ltd.

K. Janardhan Reddy is presently serving as a Professor at the School of Mechanical Engineering (SMEC), VIT University, Chennai. He has 24 years of experience in teaching and research and has published over 40 research papers in internationally reputed peer-reviewed journals in the area of product life-cycle management and new product development. He had successfully completed multiple funded projects and consultancy work to various funding agencies and industries. Presently, working in the research domains like new product development, innovation management, lifecycle management, reverse engineering.

1 Introduction

The human sensitivity to noise, vibration and harshness (NVH) is defined in the frequency scale as vibration: 1~100 Hz, harshness: 10~100 Hz, noise: 100~20 kHz, respectively. The transfer path bridges the NVH sources to the human senses. The primary function of powertrain mounts in NVH applications is to absorb and reduce force transmissibility from the powertrain to the body. So, natural rubber is widely used as an isolator to do the same. A trend towards increasing the use of polyurethane (PU)-based polymer instead of natural rubber, in powertrain mount application, especially in electric vehicles, has been observed. It is mainly because of the low dynamic stiffness property of PU material that reduces the interior noise. As EVs are more sensitive to noise from road or powertrain, the transfer path treatment is essential. Alternative material shows a better way to address typical NVH issues, especially in EVs.

Figure 1 Typical application in electric vehicle (see online version for colours)

Source: A2MAC1 Portal (2021)

PU's high volume compressibility enables us to use smaller packaging, making a product 30% lighter than a rubber material. As a result, the packaging space is also saved. The fatigue resistance improved due to compression loaded PU design against shear loaded rubber design. The interior acoustic can be improved by using low stiffening PU recipes.

The PU material has high load-bearing capability in a limited volume and abrasion resistance properties.

PU is generally used in bump stopper or jounce bumper in suspension strut. Gradually the application field extended to steering dampers, torsional dampers or pulleys: bushes, subframe mounts and engine mounts due to its low dynamic stiffening and damping properties. PU has rubber-like properties in load-deflection behaviour, which can be used as a high radial to axial stiffness ratio and high acoustic insulation demand. High linear travel and low dynamic stiffening effect can be suitable for engine mount application. A typical PU application as powertrain mounts is shown in Figure 1.

2 Literature survey

Rubber is a standard material used for various applications for NVH solutions. However, rubber has some limitations in NVH isolation properties due to its compact viscoelastic structure. However, a foam-type material is perfect for sound isolation but not durability. PU is a material that has good energy absorption capability and a low permanent set.

These properties are widely used in automotive chassis applications like bump stoppers and body mounts. With the lightweight material demand and high-performance requirement, PU-based mounts are being explored for powertrain mount application.

Qatu (2012) presented a review of recent research on NVH importance in automotive.

Yanping (2018) has discussed PU application in automobile NVH solutions in recent years. Qatu et al. (2009) presented an NVH overview on sound quality and the importance of NVH research on the early stage of vehicle design.

They have studied various materials, the current state of research, market and future applications. Prolingheuer and Henrichs (1991) have studied the microcellular PU elastomers as damping elements in automotive suspension systems. The effect of microcellular cast PU on dynamic performance and vehicle handling behaviour is studied. The advance over rubber is studied for vehicle comfort and stability requirement. The proper selection of finite element methods for predicting mechanical behaviour is also essential during the design stage. The FEA method's stratification for PU bump stopper was studied by Wang et al. (2015). In this paper, the hyper-elastic foam model is used for analysis. The bumper considered in this model is divided into three layers to study the material properties: outer skin, middle layer, and inner core. The material model coefficients are calculated by using various curve fitting methods. This study could not get the proper mechanical behaviour of the skin layer. The proposed FEA method aimed to reduce the physical prototype during actual vehicle development.

FE tools have been widely used to design the shape of bump stopper and folding pattern as discussed by Nallasamy (2007). The folding pattern is decided through FE analysis as explained in this paper for jounce bumper design based on strain rate. The hyper-elastic model for large deformation has been studied by Raja and Malayalamurthi (2011) and compared with experimental data for modelling large deformation mechanics problems. The generic design principle for durability and manufacturing aspects of various microcellular PU jounce bumpers are discussed by Dickson (2004). This paper discusses various MDI and NDI formulations, their load-deflection characteristics, and generic design parameters. The effect of various design parameters on durability is done by Dickson et al. (2005). The folding pattern, effect of retainer ring and various durability aspects consideration during the design stage are discussed in this paper.

Rogge et al. (2003) have studied the design process of MCU for body mount application. In this paper, the dynamic stiffness of MCU up to 300 Hz is compared with natural rubber. The fractional derivative viscoelastic model for rubber material is described by Lu (2007) to characterise the complex material moduli where frequency-dependent characterisation is done. At high frequency, the dynamic stiffness of MCU mounts acquires steadiness instead of continuous increase like in rubber. This property is advantageous to improve high-frequency interior sound improvement. The study of these particular low frequency and high-frequency dynamic properties are not done for powertrain mount application which is a research gap.

The material properties of damping, volume compressibility, load-deflection characteristics of MCU and their relevance for NVH applications were studied by Friedrich (2011). This paper compares the load-deflection characteristics, loss angle, and dynamic properties between rubber and MCU. Diphenylmethane diisocyanate (MDI) and Naphthylenediisocyanate (NDI)-based MCU materials are studied for NVH performance applicable for bump stopper and body mounts.

The material selection for powertrain mounts is crucial for achieving the required isolation performance. A study of the engine mount material aspect for an internal combustion engine is done by Kumar et al. (2018). Silverwood et al. (2003) have studied the improved durability, dynamic characteristics, and temperature resistance capability of microcellular urethane (MCU) in the engine mount application. This study is mainly related to developing temperature-resistant materials like MCU for engine mount applications. However, the study did not cover the NVH aspect due to the choice of MCU material.

The design approach of engine mount in an electric vehicle is studied by Hazra (2019), where the dynamic force transfer is studied for three points and four points systems with rubber mounts. There is a dearth of study of PU or MCU as materials for electric vehicle powertrain mount application.

The novelty of the work discussed in this paper lies in using PU material as a powertrain mount application and the benefit of using it for minimisation of transmitted force, especially in an electric vehicle.

This paper also discussed the improved creep and durability properties of PU over NR, which has not been addressed so far for electric powertrain mount application. The relationship between rubber and PU dynamic stiffness and the effects of low dynamic hardening properties on overall vibration transfer is discussed through a case study.

3 Powertrain mounting system in EV

Like ICE, an EV powertrain mounting system is designed to minimise the dynamic force transfer from a powertrain source to a body (passenger cabin) through an engine mount. The dynamic stiffness plays a vital role for modal separation in 6-degrees of freedom (DOF) alignment. The static stiffness is essential to hold the powertrain, and progression characteristics are responsible for transient behaviour under various torque applications. The dynamic and static stiffness ratio plays a pivotal role while selecting a powertrain mount material. The lower Kd (dynamic stiffness) / Ks (static stiffness) ratio is better for controlling structure-borne noise.

In ICE, the 1st or 1.5th order or the 2nd order powertrain excitation hinders the placement of the powertrain modes on the modal map. Sometimes, the 0.5th order issue aggravates the situation. For EV, such challenges are not there. However, the requirements of suspension modes below 5 Hz and the wheel hop modes away from 11–13 Hz need separation from EV powertrain mounts modes.

The modal targets for a four-cylinder engine are presented in Figure 2, where the 2nd order is an excitation mode. X, Y and Z directions are as per the vehicle coordinate system as mentioned in Figure 3. The powertrain modes are 6.7, 7.8, 8.5, 9.9, 10.9 and 14.4 Hz, respectively. These modes are away from suspension modes (>5 Hz), wheel hop modes (11.5~12.2 Hz) and 2nd order excitation frequency. The highest powertrain mode is separated by 11 Hz from engine excitation frequency. Similarly, the modal targets for a three-cylinder powertrain with a balancer shaft is different from that of an engine without a balancer shaft. Such excitation modes as 2nd order (26 Hz as mentioned in Figure 2) in the four-cylinder engine are not in EV. Due to the engine masking effect, the noise not there in ICE becomes predominant in EV.

Figure 2 Modal targets of a four-cylinder internal combustion engine (see online version for colours)

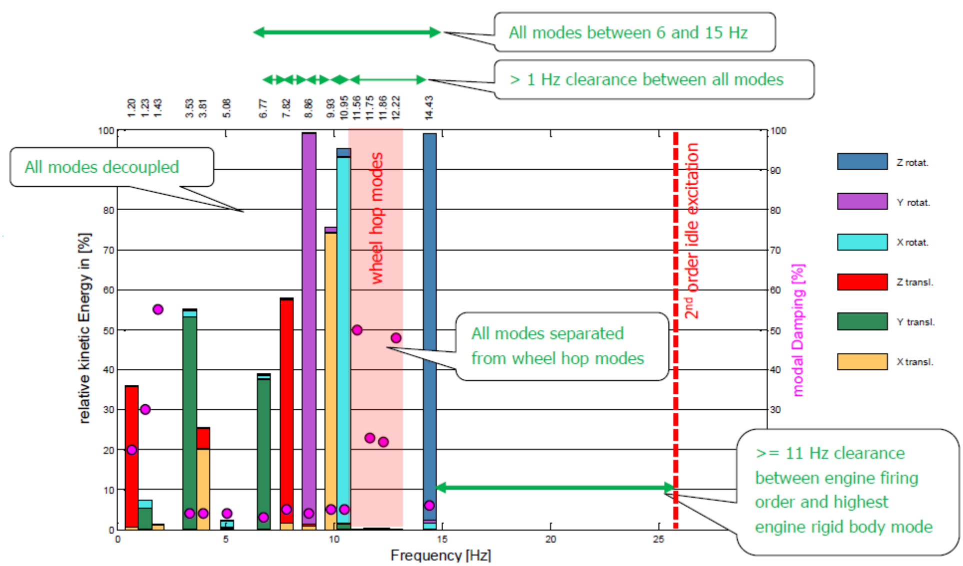

Figure 3 Vehicle coordinate system (X+ indicates the vehicle rear direction)

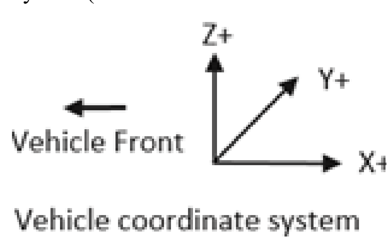

As a result, the transfer force from the powertrain to the passenger cabin requires optimisation, which is only possible by choosing a different material like PU, which has a low Kd / Ks ratio at an amplitude of +/–0.1 mm, as shown in Figure 4. For a 55 ShA rubber compound, the Kd / Ks is higher than a similar PU @ 0.55 density material. PU material and its control on compression are fundamental in achieving the static rate, progression curve, and dynamic stiffness.

Figure 4 Frequency vs. dynamic (Kd) / static (Ks) ratio comparison for NR and PU @ +/–0.1 mm amplitude (see online version for colours)

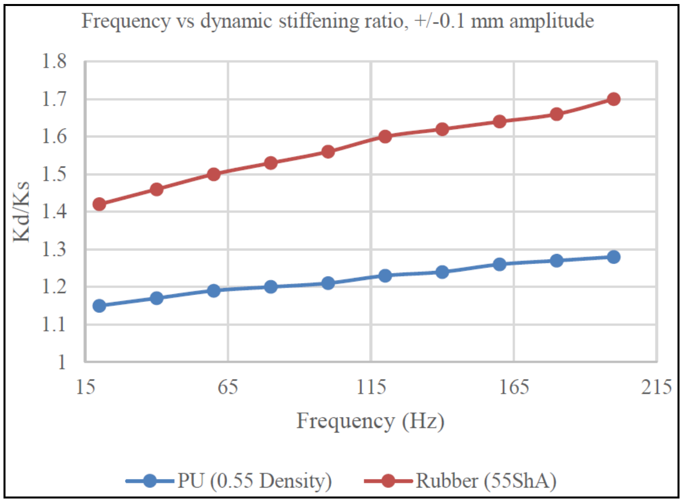

Figure 5 Loss angle vs. material at low and high amplitude (see online version for colours)

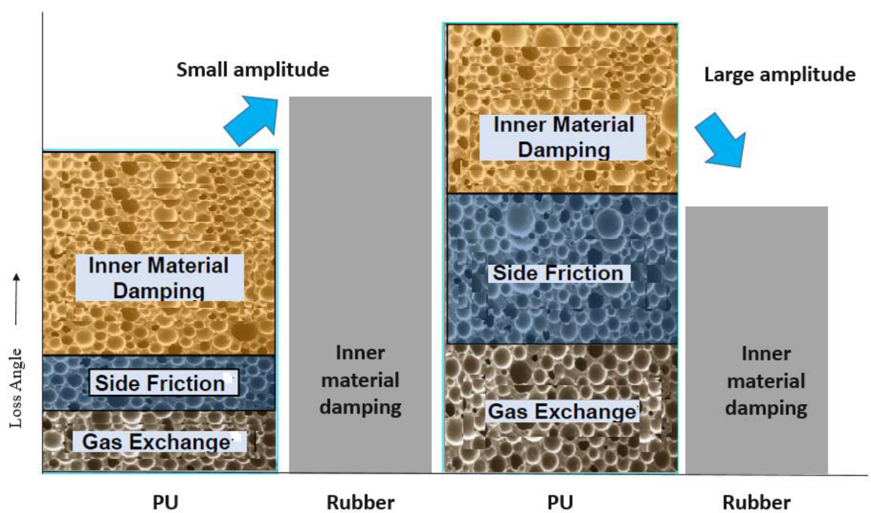

The damping behaviour for the low and high amplitude of PU and rubber is explained in Figure 5. The damping is highly influenced by amplitude. This particular property is used at high amplitude applications with more PU damping than the rubber. So, at low frequency, the dynamic stiffness of PU is used to reduce the dynamic force, and at high amplitude, the damping property is used. Similarly, at low amplitude, the loss angle of PU is lower than rubber, but at high amplitude, the loss angle is higher than rubber. The lower dynamic stiffness contributes to low in-cab noise due to minimum structure-borne noise contribution.

4 Material property of PU

The stress-strain experimental data for various densities of PU materials is shown in Figure 6 for a sample cylindrical shape with a known inner diameter (ID), outer diameter (OD) and length. PU materials of five different densities, ranging from 0.40 g/cc to 0.60 g/cc, are tested. First of all, the focus is directed on the characterisation of the PU material for the stress-strain properties.

Figure 6 Stress-strain properties of PU material at various densities (see online version for colours)

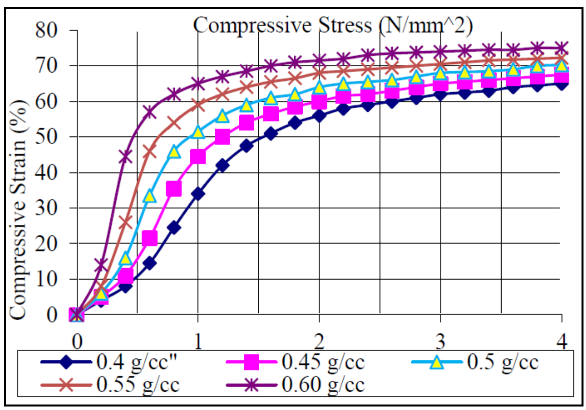

Figure 7 Test sample and testing setup (see online version for colours)

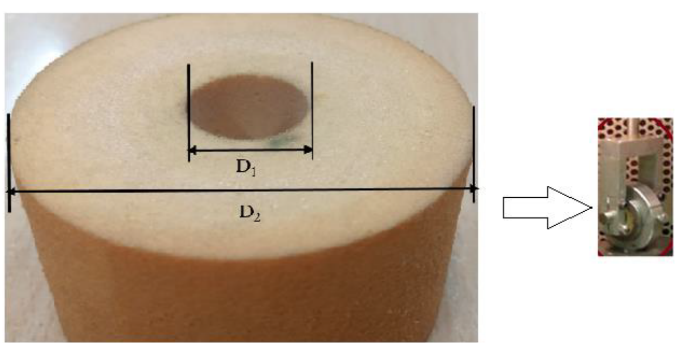

The test setup is shown in Figure 7, where a cylindrical part with known ID (D_1) and OD (D_2) was tested to generate the characteristics. The stress-strain relationship of PU elastomer is nonlinear as measured in the uniaxial compression test.

5 Comparison of creep properties

Creep is an important property of the material used in the engine mount. As engine mounts are preloaded for the vehicle's entire life, the permanent set and creep characteristics are essential parameters for overall NVH performance. If the creep is more, it can lead to stopper touching. It will result in additional transfer paths and noise issues. The actual test results of NR and PU creep behaviours are summarised in Table 1. It shows that PU material creep characteristics are better than those of NR, and the improvement level in the permanent set is around 50% for a particular mount.

$$\text{Creep } (\%) = (H_w - H_{wt}) * 100 / H_w$$

$$\text{Compression set } (\%) = (H_i - H_f) * 100 / H_i$$

where

H_i initial height of assembly without application of preload

H_w height of assembly with an application of static preload due to engine

H_{wt} height of the assembly during application of the constant load after a specified time

H_f final height of the assembly after removal of the load.

Table 1 Creep test result for NR and PU material

Time (hrs)	*Temp (°C)*	*Load (N)*		*NR*	*PU*
0	80	0	H_i	50	50
1	80	650	H_w	54.5	55
140	80	650	H_{wt}	55.05	55
150	80	650	H_f	51.5	51
Creep (mm)				1.05	0.5
Permanent set (mm)				1.5	0.5
% improvement in PU w.r.t NR				*52%*	

Figure 8 (a) Creep test machine (b) Test result – permanent set vs. time (see online version for colours)

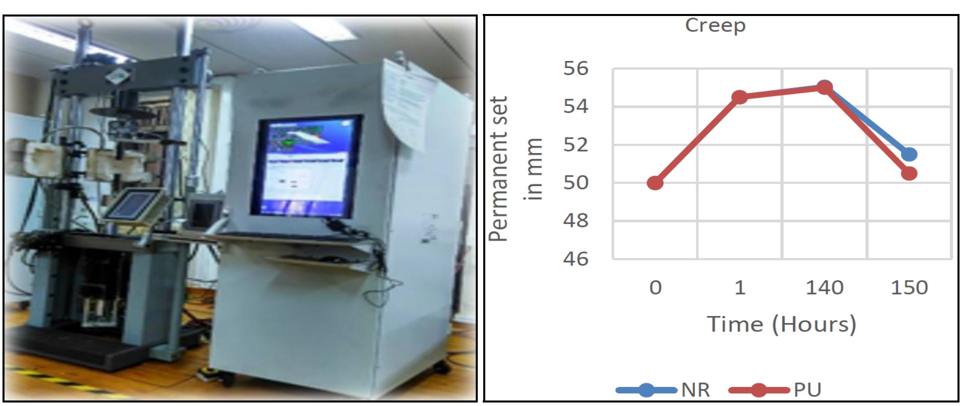

(a) (b)

In our case study, the preload applied is 650 N, which is the static preload for an electric powertrain of 136 kg. Figure 8 represents the permanent set vs. time between PU and NR material mount. PU has better permanent set properties over NR as per test data presented in Table 1. The creep testing machine setup is shown in Figure 8(a) and the test result of the permanent set is shown in Figure 8(b).

6 Comparison of durability properties

6.1 Test conditions

It is always important to focus on durability for a particular strain level to evaluate the durability performance. Strain values of 25% and 10% are considered on the test sample as per ASTM D430 – 06 (2018).

Test temperature is considered 80°C, initial notch: 1 mm, test speed 5 Hz, cycles: average of three samples are tested.

The durability check is done on a test sample created as mentioned in Figure 9(a). Three samples were tested for a strain rate of 10% and 25%. The crack growth or failure is evaluated as per ASTM D813 – 07 (2019) and ISO 132 (2017), respectively.

The dimension mentioned in Figure 9(b) is prepared for both PU and rubber material [refer to Figure 9(a)]. Then the samples are assembled in a fixture as mentioned in Figure 9(c), which is tested in De Mattia flex tester as per ASTM D430 – 06 (2018) dynamic fatigue test as shown in Figure 9(d).

Figure 9 (a) Durability test sample of NR and PU (b) Durability test sample dimension as per ASTM D430 – 06 (2018) (c) Test sample setup in fixture (d) De Mattia flex tester (see online version for colours)

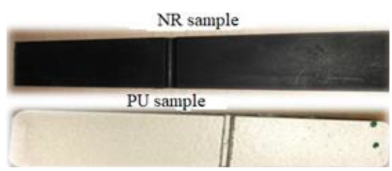

(a)

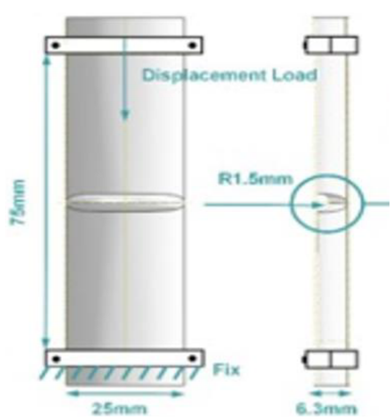

(b)

Figure 9 (a) Durability test sample of NR and PU (b) Durability test sample dimension as per ASTM D430 – 06 (2018) (c) Test sample setup in fixture (d) De Mattia flex tester (continued) (see online version for colours)

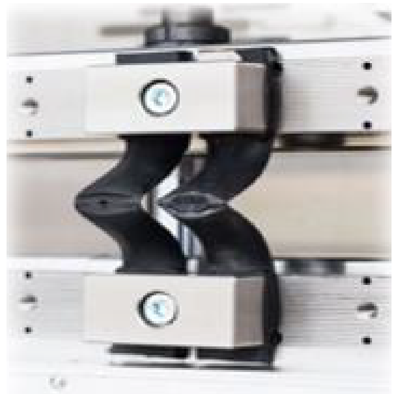

(c)

(d)

Based on the test result after the dynamic fatigue test, the durability improvement due to PU material is around 30~50% compared to NR material at different strain rates, shown in Table 2. This experimental result indicates that PU could be a better option for durability if designed meticulously for engine mount applications.

Table 2 % strain vs. no of cycle

% strain	*Number of cycles*	
	NR	*PU*
25%	6,000	8,000
10%	40,000	60,000

7 Comparison of dynamic stiffness properties

At low amplitude, the dynamic properties are compared between NR and PU and the test set-up is described in Figure 7. The low amplitude and low-frequency dynamic stiffness test results are compared for PU and NR in Figure 10, where D_1 is the ID, and D_2 is the OD of the PU bush.

The test result comparison is provided in Figure 4 for frequency vs. dynamic stiffness for an amplitude of +/–0.1 mm.

The Kd / Ks difference is more negligible between rubber and PU, as shown in Figure 10 when tested for an amplitude of +/–0.05 mm.

Figure 10 Dynamic stiffness of PU vs. rubber (see online version for colours)

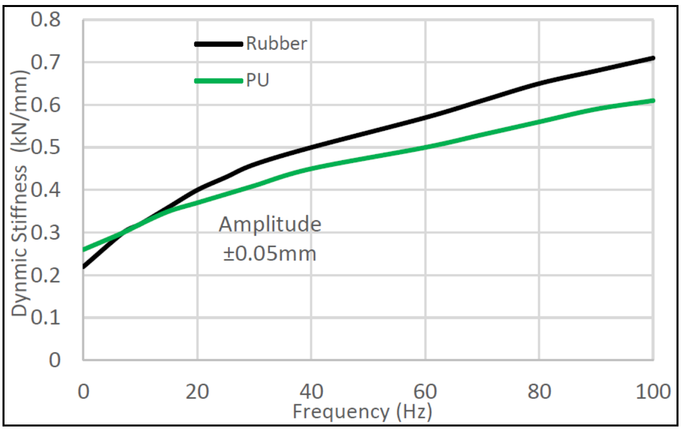

These dynamic properties of PU are used to get maximum benefit in reducing dynamic force transfer and improving noise isolation for the EV powertrain mounting system.

Dynamic properties of rubber vs PU are considered for overall system-level analysis to find out transmitted force and the effect of damping, which is discussed through a case study.

8 Case study

8.1 Input powertrain data for 6-DOF analysis

The following EV powertrain with mass, inertia, centre of gravity data, as mentioned in Table 3, is considered for 6-DOF system analysis. X, Y and Z dimensions are from the vehicle coordinate system as mentioned in Figure 3.

In this study, the powertrain properties (mass, inertia and centre of gravity) and powertrain mount locations are kept the same, whereas the powertrain mount's dynamic stiffness properties are varied based on the Kd/Ks ratio achieved in PU vs. rubber material. Without any change in static stiffness, lower dynamic stiffness achieved due to the use of PU material in place of rubber helped reduce dynamic force, which is calculated in this study. Simultaneously, the modal alignment and kinetic energy (KE) distribution at each setup were also calculated to compare the impact of PU mount vs. rubber mount's impact on electric vehicle application.

Table 3 Mass, inertia, CG data considered for analysis – rubber and PU mounts

Powertrain						
Torque (N.m)		170				
Power train mass in kg		136				
Inertia matrix (kg.m^2)						
I_{xx}		7.37				
I_{yy}		4				
I_{zz}		6.40				
I_{xy}		0.96				
I_{xz}		0.08				
I_{yz}		–1.56				
CoG mm (x, y, z)	–200	46	180			
Mount coordinate in mm (x, y, z)						
	X	Y	Z			
RH	–250	480	450			
LH	–180	–405	310			
RR	225	–55	–55			
Dynamic stiffness in N/mm (X/Y/Z)						
	Rubber mount			*PU mount*		
RH	120	120	180	85	85	135
LH	40	20	160	80	25	125
RR	135	10	10	125	10	10
Kd / Ks	1.40	1.40	1.40	1.20	1.20	1.20

Based on 6-DOF analysis with natural rubber properties, the KE distribution and eigenmodes (modes 1, 2, 3, 4, 5, 6) are calculated and presented in Figure 11(a) for rubber and Figure 11(b) for PU mount. The torque roll axis (TRA) and elastic axis (EA) alignment are shown in Figure 12(a) for rubber and Figure 12(b) for PU mount. Mount 1 and mount 2 are right side and left side mount, respectively, as mentioned in Figure 12. Tie bar 1 is the rear mount shown in Figure 12. CofG is the centre of gravity of the powertrain, and the EA is the EA. The TRA is the function of powertrain mass, inertia, CofG, and EA is the function of powertrain mounts static stiffness. The relative location of TRA and EA gives a vital indication about idle force transfer during torque reaction in the mounting system. The ideal design involves these two axes are to be coincident.

The TRA and EA are not aligned as mentioned in Figure 12(a) for rubber mounts, and as a result, the modal energy decupling is not pure, as shown in Figure 11(a). There is a significant coupling between yaw and roll at 9.2 and 12.6 Hz, respectively. The ideal requirement of TRA and EA should be <1°, and the KEE should be >90% for an optimised system.

Figure 11 6-DOF KE and rigid body modes, (a) rubber mounts (b) PU mounts (see online version for colours)

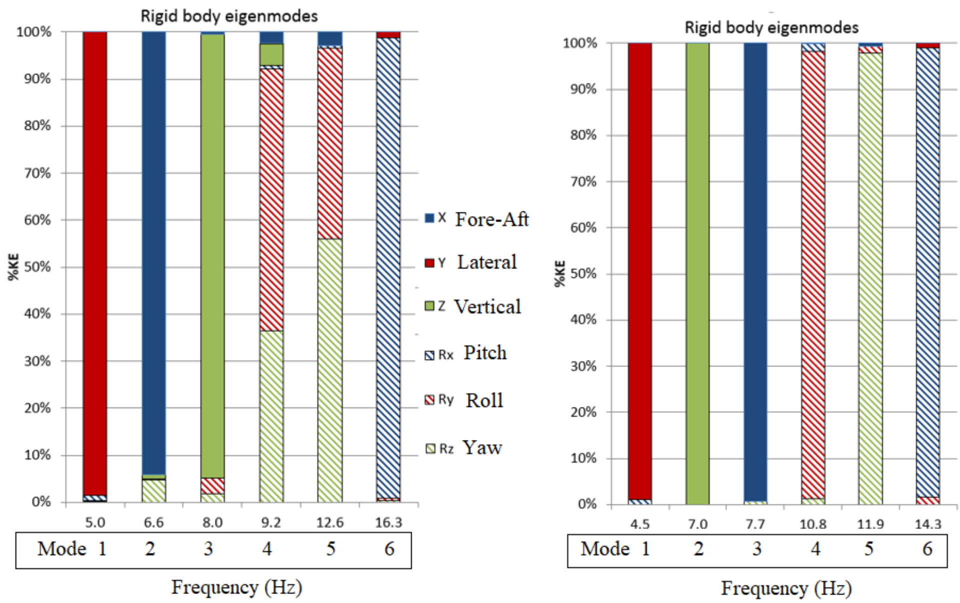

(a) (b)

Figure 12 TRA – EA location on Y-Z plane, (a) rubber mounts (b) PU mounts (see online version for colours)

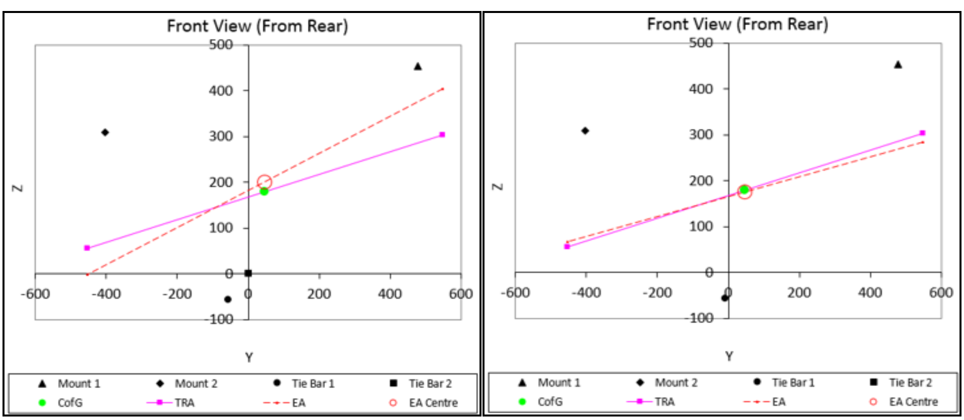

(a) (b)

8.2 *With PU mounts*

The PU mount setup with lower dynamic stiffness have good TRA and EA alignment [Figure 12(b)] and also have good modal alignment, and all modes are decoupled to each other. The stiffness of PU mounts in all directions are mentioned in Table 3. The rest of the powertrain properties (mass, inertia and centre of gravity) are considered unchanged.

Then the 6-DOF calculation was carried out to check the modal alignment and KEE coupling. The TRA and EA alignment are also checked. The TRA and EA have perfect alignment, as mentioned in Figure 12(b), and as a result, the modal energy decupling is also achieved.

The TRA and EA alignment is much better with a lower Kd / Ks ratio, achievable through PU mounts. Figure 12(b) shows the alignment is <1°, whereas Figure 12(a) shows that the alignment is around 4°. Similarly, the KEE distribution for PU mounts is much better than rubber mounts because of its low Kd / Ks ratio. The lower dynamic stiffness resulted in the maximum modal value in PU setup as 14.3 Hz, lower than rubber setup, i.e., 16.4 Hz.

The dynamic force is calculated for both the materials to compare the impact through analytical calculation and modelling.

9 Analytical model for calculation of force transfer

The EV powertrain unit is considered a 1D model, as described in Figure 13.

The viscoelastic elements are considered with effective inertia. The powertrain is assumed as a lumped mass, and all three mounts are spring-mass systems, as mentioned in Figure 13. The motion is considered in one direction for the model's simplicity and easy comparison. A forced vibration response is applied to the system with a specific force exerted on the powertrain unit. The dynamic response of the powertrain system is analysed in the frequency domain by changing loss angle values. The value of loss angle is evaluated as 0, 5, 10 and 15°, respectively.

Figure 13 1D model of three-point mounting system (see online version for colours)

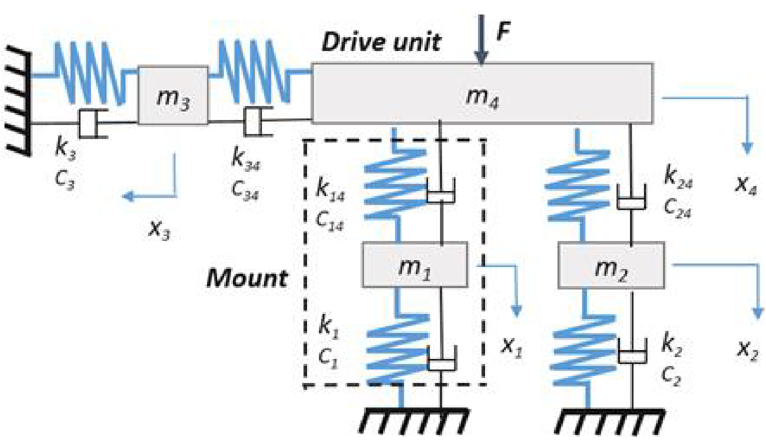

Model assumption:

a Here, the powertrain unit is considered analysed as a 1D model.

b All three mounts are considered spring-mass systems attached to the powertrain unit and represented in a simplified spring-mass system.

c The motion is considered only in the vertical direction for simplification of analysis.

d The system is considered as a forced vibration system where the force is applied to drive unit.

e Frequency domain analysis is conducted to analyse the system response.

f Mounting mass is also considered in spring, mass system to evaluate the mass effect.

Let, F is applied force on EV powertrain unit of mass m_4. The mass effect of all three mounts is considered m_1, m_2 and m_3, respectively. k_1, k_{14}, k_2, k_{24}, k_3, k_{34} are stiffness values, C_1, C_{14}, C_2, C_{24}, C_3, C_{34} are damping values, whereas $x_{1,2,3,4}$ are the corresponding displacement.

The equations from the free body diagram the governing equation become as below:

$$\begin{bmatrix} -m_1 & \omega^2 & 0 & 0 & 0 \\ 0 & -m_2 & \omega^2 & 0 & 0 \\ 0 & 0 & -m_3 & \omega^2 & 0 \\ 0 & 0 & 0 & -m_4 & \omega^2 \end{bmatrix} \begin{Bmatrix} x_1 \\ x_2 \\ x_3 \\ x_4 \end{Bmatrix} + [C] \begin{Bmatrix} \dot{x}_1 \\ \dot{x}_2 \\ \dot{x}_3 \\ \dot{x}_4 \end{Bmatrix} + [k] \begin{Bmatrix} x_1 \\ x_2 \\ x_3 \\ x_4 \end{Bmatrix}$$
$$= \begin{Bmatrix} 0 \\ 0 \\ 0 \\ F \end{Bmatrix} (z(\omega)) \begin{Bmatrix} x_1 \\ x_2 \\ x_3 \\ x_4 \end{Bmatrix} = \begin{Bmatrix} 0 \\ 0 \\ 0 \\ F \end{Bmatrix} \tag{1}$$

$$\begin{Bmatrix} x_1 \\ x_2 \\ x_3 \\ x_4 \end{Bmatrix} = \left(z(\omega)^{-1}\right) \begin{Bmatrix} 0 \\ 0 \\ 0 \\ F \end{Bmatrix} \tag{2}$$

$$\begin{Bmatrix} x_1 \\ x_2 \\ x_3 \\ x_4 \end{Bmatrix} = \frac{\operatorname{adj}(z(\omega)) \begin{pmatrix} 0 \\ 0 \\ 0 \\ F \end{pmatrix}}{\lfloor z(\omega) \rfloor} \tag{3}$$

The mounting system transmissibility is the magnitude of excitation force transmitted through the mount to the long member for a given excitation frequency. Moreover, this is calculated and compared for all three mounts.

The transmitted force is simulated for the right, left, and rear mount. The calculated transmitted for various loss angles of 1°, 5°, 10° and 15° are calculated for rubber. The same is presented in Figure 14(a) where it is established that the transmitted force is reduced while increasing the loss angle. We aim to check whether rubber material can reduce the transmitted force like PU. For that, the transmitted force is calculated for PU material also. The calculated values for 1° loss angle is presented in Figure 16(b). It shows that the minimum loss angle of 1° of PU has transmitted 933 N at 7.5 Hz, whereas it is 2,081 N for rubber material with a higher loss angle of 15°. It is due to the low dynamic stiffness that can be achieved for PU compared to rubber. The Z-direction transmitted force has a peak at 7.5 Hz frequency close to the bounce mode (7.7 Hz) mentioned in Figure 11(b) of the overall system.

Figure 14 (a) Right side mount-transmitted force of rubber mount vs. loss angle (b) Transmitted force of rubber and PU mount for 1° loss angle (see online version for colours)

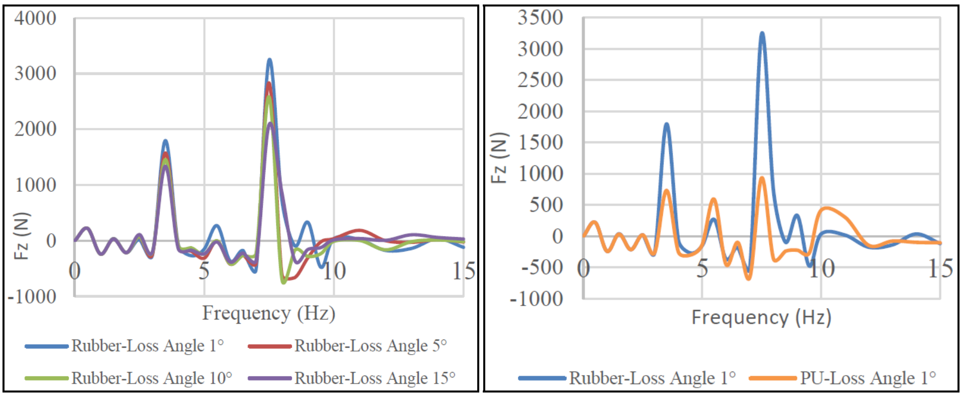

(a) (b)

A similar study for the left side mount [presented in Figures 15(a) and 15(b)] is carried out. PU with a 1° loss angle has transmitted force 1,179 N at 7.5 Hz, which is less than rubber material (1,381 N) even with a higher loss angle of 15°.

Figure 15 (a) Left side mount-transmitted force of rubber mount vs. loss angle (b) Transmitted force of rubber and PU mount for 1° loss angle (see online version for colours)

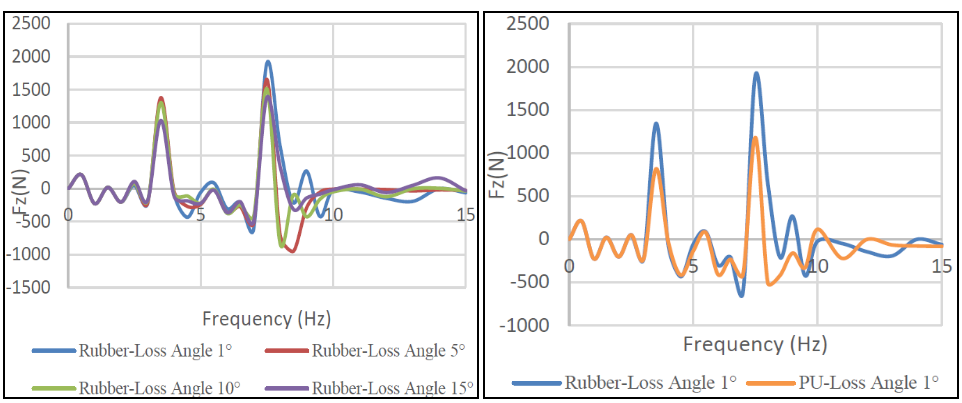

(a) (b)

Similarly, for the rear mount, the transmitted force in the X-direction with PU material is less than that of rubber material. Figure 16 shows the overall force transfer for a PU mount compared to a rubber mount at a loss angle of 1°.

In almost all cases, the transmitted force with PU mounts is lower than the rubber mount, which benefits vibrations transfer for a particular loss angle.

Figure 16 Rear mount-transmitted force of rubber and PU mount for 1° loss angle (see online version for colours)

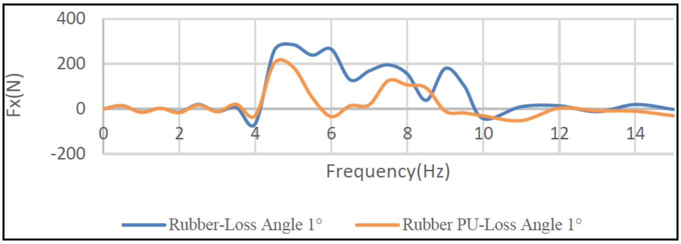

The amount of transmitted force is compared between rubber and PU material for the same input but with various damping values. The Z-direction transmitted forces are significantly reduced in PU than rubber mount for the same input, as mentioned in summary Table 4. The reduction in Z-direction transmitted force benefits the force transmissibility and thus improves NVH performance. The calculation is done for the right-hand side (RHS), left-hand side (LHS) mount Z-direction and rear mount X-direction force. The loss angle also varied to check the impact of material damping.

Table 4 Comparison of dynamic forces on RHS, LHS and rear mounts for rubber and PU with various damping factors (loss angle)

Loss angle	*1°*	*5°*	*10°*	*15°*	*Material*
RHS force in (N)	933	799	716	665	PU
	3,240	2,833	2,581	2,081	Rubber
LHS force in (N)	1,179	1,019	924	912	PU
	1,901	1,656	1,513	1,381	Rubber
Rear force in (N)	185	86	78	22	PU
	285	35	33	25	Rubber

Figure 17 Simulated noise level with frequency for rubber and PU mount stiffness (see online version for colours)

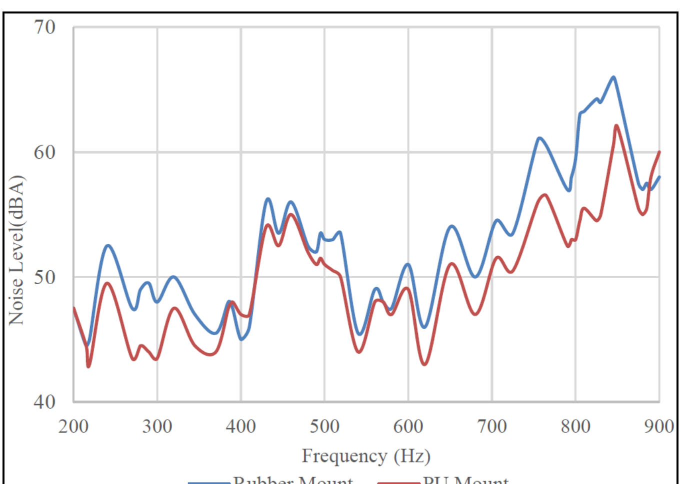

There is a considerable difference between the dynamic stiffness values of NR compared to PU because of their material property that gives better isolation at small amplitudes. It means the road noise isolation is better for PU mounts.

The vehicle level noise differences between rubber and PU mounts are also estimated for rubber and PU stiffness. As mentioned in Figure 17, the overall vehicle level noise also reduces for lower mount dynamic stiffness, which can be achieved by suitable design and PU material application.

10 Conclusions

The use of PU-based material for engine mount application in an electric vehicle is established to be promising for the improvement of overall NVH characteristics. The low dynamic stiffening factor reduces the dynamic force transfer from the active to the passive side of powertrain mounts.

The impact of loss angle on force transfer is calculated and presented for PU vs. rubber material. The force transfer with PU material is much lower than rubber material. The overall noise is also reduced when PU is substituted for rubber.

The study of dynamic properties creep, and durability gives a directional framework for the usage of PU mount in the electric vehicle.

Due to inferior temperature resistance properties, it is challenging to use PU in the ICE powertrain. However, the same challenges are not there in EV.

The significant impediments in PU application in engine mount are designing the shape factor properly to meet durability and progression requirements. With the right design, it is possible to achieve the superior property of PU compared to rubber for engine mount application in an electric vehicle.

References

A2MAC1 Portal (2021) [online] https://portal.a2mac1.com/ (accessed 9 August 2021).

ASTM D430 – 06 (2018) *Standard Test Methods for Rubber Deterioration – Dynamic Fatigue*.

ASTM D813 – 07 (2019) *Standard Test Method for Rubber Deterioration – Crack Growth.*

Dickson, D. (2004) *A Primer on Jounce Bumper Design Using Microcellular Polyurethane*, SAE Technical Paper.

Dickson, D., Schranz, S. and Wolff, M. (2005) *Microcellular Polyurethane Jounce Bumper Design and the Effects on Durability*, SAE Technical Paper.

Friedrich, F. (2011) *Microcellular Polyurethane (MCU) for NVH Solutions*, SAE Technical Paper, No. 2011-01-1621.

Hazra, S. (2019) *Engine Mounting System Design Approach for Electric Vehicles*, SAE Technical Paper.

ISO 132 (2017) *Rubber, Vulcanized or Thermoplastic – Determination of Flex Cracking and Crack Growth (De Mattia)*.

Kumar, D.S., Reddy, M.R., Vijayarangam, J., Virinchy, C.S. and Asif, A.H. (2018) 'Studies on design and material aspects of IC engine mounts for vibration reduction', *International Journal of Pure and Applied Mathematics*, Vol. 118, No. 9, pp.355–366.

Lu, Y.C. (2017) 'Fractional derivative viscoelastic model for frequency-dependent complex moduli of automotive elastomers', *International Journal of Mechanics and Materials in Design*, Vol. 3, No. 4, pp.329–336.

Nallasamy, S.H. (2007) 'Jounce bumper optimization – FE approach', *Abaqus Conference*.

Prolingheuer, C. and Henrichs, P. (1991) *Microcellular: Polyurethane Elastomers as Damping Elements in Automotive Suspension Systems*, SAE Technical Paper Series.

Qatu, M.S. (2012) 'Recent research on vehicle noise and vibration', *International Journal of Vehicle Noise and Vibration*, Vol. 8, No. 4, pp.289–301.

Qatu, M.S., Abdelhamid, M.K., Pang, J. and Sheng, G. (2009) 'Overview of automotive noise and vibration', *International Journal of Vehicle Noise and Vibration*, Vol. 5, Nos. 1–2, pp.1–35.

Raja, K.V. and Malayalamurthi, R. (2011) 'Assessment on assorted hyper-elastic material models applied for large deformation soft finger contact problems', *Int. J. Mech. Mater. Des*., Vol. 7, No. 4, p.299.

Rogge, T., Silverwood, H. and Love, M. (2003) *MCU Optimization in Body Mount Applications*, SAE Technical Paper.

Silverwood, H., Klufts, E. and Rogge, T. (2003) *Temperature Resistant Microcellular Polyurethane For Engine Mounting Applications*, SAE Technical Paper, No. 2003-01-1582.

Wang, Y., Ma, Z. and Wang, L. (2015) 'A finite element stratification method for a polyurethane jounce bumper', *Proceedings of the Institution of Mechanical Engineers*, Vol. 230, No. 7, pp.983–992.

Yanping, Y. (2018) 'The development of polyurethane. Materials science', *Materials Review*, Vol. 1, No. 1, pp.1–8.